Peristaltic pumping through non-Darcy porous medium in an electroosmotic flow with entropy analysis

Bhimanand Pandurang Gajbhare[1,2], J. S. V. R. Krishna prasad[3], S. R. Mishra[4]

[1]Research Scholar, Kavayitri Bahinabai Chaudhari North Maharashtra University, Jalgaon, India
[2]Department of Mathematics, Vaidyanath College Parli-Vaijanath, Beed-431515, Maharashtra, India
[3]Department of Mathematics, Moolji Jaitha College, Jalgaon-425001, Maharashtra, India
[4]Department of Mathematics, Siksha O Anusandhan Deemed to be University, Khandagiri square, Bhubaneswar-751030, Odisha, India

bpgajbhare@gmail.com, krishnaprasadjsvr@yahoo.com, satyaranjan_mshr@yahoo.co.in

Pumping of peristaltic fluid is a vehicle via liquid that is accomplished due to a dynamic rush through a distensible cylinder containing liquids which extends along its length. Peristaltic pumping occurs in a lower pressure region to a higher pressure region. As a principle of peristaltic pumping, various applications are used for the blood pumping in different parts of the human body, pharmacological drug delivery systems and in industries, sanitary fluid transport, etc. Therefore, peristaltic pumping via a non-Darcy porous medium in an electroosmotic flow has been discussed in the current investigation. To exhibit the existence of a porous medium, Darcy Forchheimer model is deployed. The electro-magnetohaydrodynamic flow of fluid passing a symmetric channel and the novelty of the study are due to the entropy analysis. Analytical approach such as perturbation technique is employed to reduce the higher order coupled transformed equation into its lower order decoupled form and then numerical treatment is made to obtain the approximate solutions. The characteristics of the contributing parameters are presented via graphs and the numerical computations are exhibited through tabular form. Present outcome warrants a good correlation with earlier result in particular case. However, the main findings are elaborated in the results and discussion section.

Keywords: electroosmotic flow, peristaltic pumping, Darcy–Forchheimer model; approximate analytical method, perturbation technique.

1. Introduction

The development of entropy is a phenomenon of material that is related to the degree of randomness in the system. Moreover, from the second law of thermodynamics, entropy of the system increases due to the irreversible process related to in real time. When entropy output takes place, then energy norm/status decreases. Therefore, it is of vital importance to record the distribution of entropy production in the fluid to maintain the energy norm/status during fluid flow or to minimize entropy production. Proficient energy consumption during the construction of thermal devices is the primary objective. This goal may be achieved by reducing the generation of entropy in thermodynamic processes. Entropy processing is viewed as a suitable solution with the growth of industry and improved engineering capabilities to achieve more efficiency in industrial processes. The lost resources cannot be recovered but steps for the irreversibility can be taken. The pioneering work of Bejan [1] is for implementing this concept through the minimization of entropy output. Afterwards, Sciacovelliet al. [2] introduced the study of entropy output as a design method. Zhao and Liu [3] revealed the production of entropy in open-and close-ended microconduct for the electro-kinetically flowing stream. Rashidi et al. [4] enlightened the development of entropy in a rotating disc for a steady flow with porous material. Afridi et al. [5] studied the analysis of entropy in a MHD stagnation point flow (boundary layer) for the behavior of Joule and friction heating. Gull et al. [6] carried out the amount of production of entropy of MDJN (molybdenum disulfide Jeffrey nanofluid) mixed convection Poiseuille flow, and recorded that the effects of pressure gradient and buoyancy in the mixed convection. Saqib et al. [7] examined the same amount of entropy in an electrically conducting nanofluid of different forms traveling on an infinite length vertical plate embodying with porous medium. Due to its immense applications in electronics cooling systems, nuclear reactors, and heat exchangers, the natural convection cycle inside the channel walls is a key attraction to the researchers in the last few decades. The efficient use of energy and the best possible use of resources prompted inquiries to improve the efficiency of industrial procedures. Several recent studies are reported [8–14] which explore the results of entropy analysis. Because of the vast applications in several industries, micro-fluids have gained considerable attention over the last few decades. The young academicians have used electrokinetic-based micro-fluids as it is very a powerful mechanism for manipulating and regulating the fluid flow in micro-devices. Microfluidics is also important in biofluids like concentration of DNA,

isolation of species, and fluid amalgamation. This can be used to analyze various biological properties. Coulomb force induces the electroosmotic flow through the micro-channel, driven by the electric potential. Electroosmosis is the counter-ions movement in the diffused portion of the double-layer current. This process of electroosmotic fluid flowing by peristaltic pumping in a non-Darcy porous medium, as it can be used in hemodialys is, is a very physiological significant test. Cameselle and Reddy [15] focused on advancing and developing the electroosmotic flow to remove pollution from soil. Zhou et al. [16] have been researching how electroosmotic processes are influenced by electrode material. With the impact of magnetic field, Tripathi et al. [17] studied the peristaltic motion of electrically driven fluids.

Aforesaid literature review suggests a way to study on the entropy analysis of the electro-magnetohydrodynamics flow and electroosmotic flow in a symmetric channel via non-Darcy porous medium. Darcy–Forchheimer model is considered for the present investigation. Approximate analytical technique, such as perturbation technique along with numerical technique is employed to handle the transformed non-dimensional coupled form of equations. Further, the flow phenomena along with the analysis of entropy generation are obtained by discussing the characterizing parameters via graphs and tables.

2. Mathematical model

The problem considered in the present investigation is based on the Darcy Forchheimer model for the flow characteristics of peristaltic pumping accompanied by electroosmos is via a non-Darcy porous matrix.A flow of viscous two-dimensional fluid passes in a micro channel wall with temperature T_w, where the bulk fluid temperature is denoted as T. The wave propagation occurs along $\overline{x}$ direction and the normal direction to the flow is along $\overline{y}$. It is noteworthy that, about the middle area of the conduit the flow is symmetric, i.e., $\overline{y} = 0$, which is equidistant from the upper, as well as, from the lower boundaries of the conduit $\overline{y} = \overline{h}(\overline{x}, \overline{t})$ and $\overline{y} = -\overline{h}(\overline{x}, \overline{t})$ respectively (Fig. 1). Moreover, due to symmetric flow, it is sufficient to discuss the flow phenomena within the domain $0 \leq \overline{y} \leq h$. An electric field of strength E_0 is exerted along the parallel direction of the micro-channel and magnetic field of strength B_0, which is applied in the transverse direction of the flow.
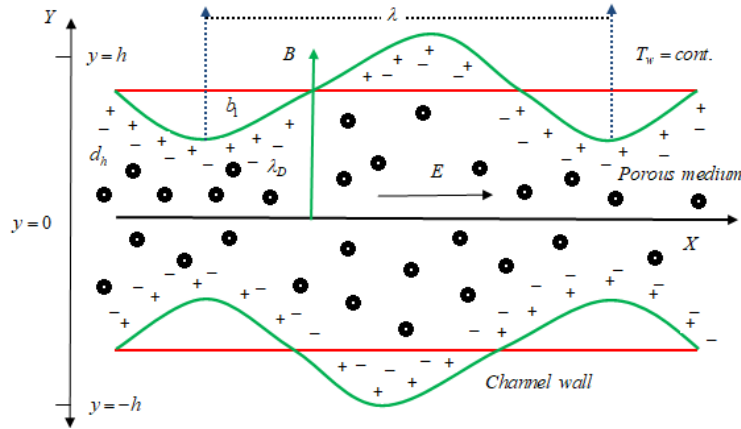

FIG. 1. Flow configuration of peristaltic pumping

Here,

$$\overline{h}(\overline{x}, \overline{t}) = d_h - \overline{b}_1 \cos^2 \frac{\pi}{\lambda}(\overline{x} - c_1\overline{t}),$$ (1)

where d_h, the half-width of the channel, λ, the wavelength, b_1, the amplitude, and c_1, velocity of the wave.

2.1. Electrical potential distribution

The electric potential in the symmetric channel is imposed following, the Poisson–Boltzmann equation and described as:

$$\nabla^2 \overline{\phi} = -\frac{\rho_e}{\varepsilon \varepsilon_0},$$ (2)

and the ion within the double layer is also proportional to Boltzmann factor $e^{-z_e \overline{\phi}/K_B T_{av}}$. Where $\overline{\phi}$, the potential of electroosmotic flow, ρ_e, density of ionic charge, ε, constant(dielectric), and ε_0 permeability. The value of ε_0 is $8.854 \times 10^{-12} Fm^{-1}$.

From the Boltzmann equation, both the positive and negative ions number densities are:

$$n^{\pm} = n_0 e^{(\mp z_e \overline{\phi} K_B T_{av})}, \tag{3}$$

Where n_0, the average of both then negative and positive ions obtained from buffer solution, z, the ionic valence, e, the charge of electron, T_{av}, the average temperature, and K_B, the Boltzmann constant. Following [19], the total charge is considered as:

$$\rho_e = ez(n^+ - n^-) = -2n_0 ez \sinh \left(\frac{ez\overline{\phi}}{K_B T_{av}} \right). \tag{4}$$

Therefore, from Eqs. (3) and (4) the Poisson–Boltzmann Eq. (2) is approximated as:

$$\frac{d^2 \overline{\phi}}{d\overline{y}^2} = \frac{-2n_0 ez}{\varepsilon \varepsilon_0} \sinh \left(\frac{ez\overline{\phi}}{K_B T_{av}} \right). \tag{5}$$

In general, introduced the following dimensionless variables for the governing equations are

$$\begin{cases} \delta = \dfrac{d_h}{\lambda}, \quad Re = \dfrac{\rho c_1 d_h}{\mu}, \quad \beta = \dfrac{U_{HS}}{c_1}, \quad U_{HS} = \dfrac{E_0 \varepsilon \varepsilon_0 \zeta}{\mu}, \quad \nu = \dfrac{\mu}{\rho}, \quad H_m = B_0 d_h \sqrt{\dfrac{\sigma}{\mu}}, \quad \Omega^2 = \dfrac{d_h^2}{k^*}, \\[3mm] \varphi = \dfrac{\overline{\varphi}}{\zeta}, \quad y = \dfrac{\overline{y}}{d_h}, \quad x = \dfrac{\overline{x}}{\lambda}, \quad t = \dfrac{c_1 \overline{t}}{\lambda}, \quad h = \dfrac{\overline{h}}{d_h}, \quad b_1 = \dfrac{\overline{b_1}}{d_h}, \quad \theta = \dfrac{T - T_w}{\frac{q d_h}{k}} p = \dfrac{\overline{p} d_h^2}{c_1 \lambda \mu}, \quad u = \dfrac{\overline{u}}{c_1}, \\[3mm] v = \dfrac{\overline{v}}{c_1 \delta}, \quad C_F = c_{k^*} \dfrac{c_1 d_h^2}{\nu k^*}, \quad \Pr = \dfrac{\mu C_p}{K}, \quad Br = \dfrac{\mu c_1^2}{q d_h}, \quad \gamma = \dfrac{\sigma d_h E_0^2}{q}. \end{cases} \tag{6}$$

With the help of non-dimensional quantities as well as variables from equation (6), equation (5) becomes:

$$\frac{d^2 \varphi}{dy^2} = \frac{d_h^2}{\lambda_D^2 \alpha} \sinh(\alpha \varphi), \tag{7}$$

where α is the ionic energy parameter, λ_D is the Debye length.

Across the middle of the channel, the potential function is symmetric therefore, the boundary conditions are:

$$\begin{cases} \dfrac{d\varphi}{dy} = 0, \quad \text{at } y = 0; \\[3mm] \varphi = 1, \qquad \text{at } y = h. \end{cases} \tag{8}$$

The solution of equation (7), with their corresponding boundary conditions (8) can be stated as:

$$\phi = \frac{\cosh(my)}{\cosh(mh)}. \tag{9}$$

Here, m is the electroosmotic parameter where $m = d_h / \lambda_D$.

3. Flow analysis

Flow of electroosmotic fluid by the peristaltic pumping in a non-Darcy porous medium can be modeled as:

$$\frac{\partial \overline{u}}{\partial \overline{x}} + \frac{\partial \overline{v}}{\partial \overline{y}} = 0, \tag{10}$$

$$\rho \left(\frac{\partial \overline{u}}{\partial \overline{t}} + \overline{u} \frac{\partial \overline{u}}{\partial \overline{x}} + \overline{v} \frac{\partial \overline{u}}{\partial \overline{y}} \right) = -\frac{\partial \overline{p}}{\partial \overline{x}} + \mu \left(\frac{\partial^2 \overline{u}}{\partial \overline{x}^2} + \frac{\partial^2 \overline{u}}{\partial \overline{y}^2} \right) - \sigma \overline{B}_0^2 \overline{u} + \rho E_0 - \frac{\mu}{k^*} \overline{u} - \frac{\rho c_{k^*}}{\sqrt{k^*}} \overline{u} \sqrt{\overline{u}^2 + \overline{v}^2}, \tag{11}$$

$$\rho \left(\frac{\partial \overline{v}}{\partial \overline{t}} + \overline{u} \frac{\partial \overline{v}}{\partial \overline{x}} + \overline{v} \frac{\partial \overline{v}}{\partial \overline{y}} \right) = -\frac{\partial \overline{p}}{\partial \overline{y}} + \mu \left(\frac{\partial^2 \overline{v}}{\partial \overline{x}^2} + \frac{\partial^2 \overline{v}}{\partial \overline{y}^2} \right) - \frac{\mu}{k^*} \overline{v} - \frac{\rho c_{k^*}}{\sqrt{k^*}} \overline{v} \sqrt{\overline{u}^2 + \overline{v}^2}, \tag{12}$$

$$\rho c_p \left(\frac{\partial \overline{T}}{\partial \overline{t}} + \overline{u} \frac{\partial \overline{T}}{\partial \overline{x}} + \overline{v} \frac{\partial \overline{T}}{\partial \overline{y}} \right) =$$

$$K \left(\frac{\partial^2 \overline{T}}{\partial \overline{x}^2} + \frac{\partial^2 \overline{T}}{\partial \overline{y}^2} \right) + \phi + \sigma \overline{B}_0^2 \overline{u}^2 + \sigma E_0^2 + \frac{\mu}{k^*} \left(\overline{u}^2 + \overline{v}^2 \right) - \frac{\rho c_{k^*}}{\sqrt{k^*}} \left[\left(\overline{u}^2 + \overline{v}^2 \right) \sqrt{\overline{u}^2 + \overline{v}^2} \right], \tag{13}$$

$$\phi = \mu \left[2 \left(\frac{\partial \overline{u}}{\partial \overline{x}} \right)^2 + 2 \left(\frac{\partial \overline{v}}{\partial \overline{y}} \right)^2 + \left(\frac{\partial^2 \overline{v}}{\partial \overline{x}^2} + \frac{\partial^2 \overline{v}}{\partial \overline{y}^2} \right) \right]. \tag{14}$$

In equation (11) the first term is pressure gradient, second term is inertia force, third and fourth terms are the magnetic and electric fields respectively, fifth term is the porosity and the sixth term is the use of drag force. For equation (13), the first term of the right hand side is the pressure gradient, second term is inertia force, third term is

porosity, and fifth term is drag force. Similarly, forequation (14), first term of right hand side is thermal diffusion, second term is viscous dissipation, third and fourth terms are the Joule dissipations due to magnetic and electric field, fifth term is Darcy dissipation due to the inclusion of porosity and the last term is drag force.

Where φ represents the inclusion of viscous dissipation in the pumping process.

Implementing (6) on the governing equations (11)–(13) using equation (14) the transformed equations are expressed as:

$$Re\delta \left(\frac{\partial}{\partial t} + u\frac{\partial}{\partial x} + v\frac{\partial}{\partial y} \right) u = -\frac{\partial p}{\partial x} + \left(\delta^2 \frac{\partial^2 u}{\partial x^2} + \frac{\partial^2 u}{\partial y^2} \right) - \left(H_m^2 + \Omega^2 \right) u + \beta m^2 \phi - c_F u \sqrt{u^2 + \delta^2 v^2}, \quad (15)$$

$$Re\delta^3 \left(\frac{\partial}{\partial t} + u\frac{\partial}{\partial x} + v\frac{\partial}{\partial y} \right) v = -\frac{\partial p}{\partial x} + \delta^2 \left(\delta^2 \frac{\partial^2 v}{\partial x^2} + \frac{\partial^2 v}{\partial y^2} \right) - \delta^2 \left(\Omega^2 \right) v + \beta m^2 \phi - \delta^3 c_F uv \sqrt{u^2 + \delta^2 v^2}, \quad (16)$$

$$Re\Pr\delta \left(\frac{\partial}{\partial t} + u\frac{\partial}{\partial x} + v\frac{\partial}{\partial y} \right) \theta =$$
$$\left(\delta^2 \frac{\partial^2 \theta}{\partial x^2} + \frac{\partial^2 \theta}{\partial y^2} \right) + \gamma + Br \left[2\delta^2 \left(\frac{\partial u}{\partial x} \right)^2 + 2\delta^2 \left(\frac{\partial v}{\partial x} \right)^2 \right] - \delta^2 \left(\Omega^2 \right) v + \beta m^2 \varphi - \delta^3 c_F uv \sqrt{u^2 + \delta^2 v^2}. \quad (17)$$

In the case of long wave length and low Reynolds number i.e. neglecting the term containing δ, the above expression can be represented as:

$$\frac{\partial p}{\partial x} = \frac{\partial^2 u}{\partial y^2} - (H^2 + \Omega^2)u + \beta m^2 \varphi - C_F u^2, \quad (18)$$

$$\frac{\partial p}{\partial y} = 0, \quad (19)$$

$$\frac{\partial^2 \theta}{\partial y^2} + \gamma + Br \left(\frac{\partial u}{\partial y} \right)^2 + (H^2 + \Omega^2)Bru^2 - C_F Bru^3 = 0. \quad (20)$$

Eliminating pressure gradient from the dimensionless equations (18) and (19), the equation for flow of electroosmotic fluid can be written as:

$$\frac{\partial^3 u}{\partial y^3} - (H^2 + \Omega^2)\frac{\partial u}{\partial y} + \beta m^2 \frac{\partial \varphi}{\partial y} - C_F \frac{\partial u^2}{\partial y} = 0. \quad (21)$$

Now,we define the stream function ψ, such as $u = \frac{\partial \psi}{\partial y}$, $v = -\frac{\partial \psi}{\partial x}$ satisfying the continuity equation (10). Equations (18), (20) and (21) can be written as:

$$\frac{\partial p}{\partial x} = \frac{\partial^3 \psi}{\partial y^3} - (H^2 + \Omega^2)\frac{\partial \psi}{\partial y} + \beta m^2 \varphi - C_F \left(\frac{\partial \psi}{\partial y} \right)^2, \quad (22)$$

$$\frac{\partial^2 \theta}{\partial y^2} + \gamma + Br \left(\frac{\partial^2 \psi}{\partial y^2} \right)^2 + (H^2 + \Omega^2)Br \left(\frac{\partial u}{\partial y} \right)^2 - C_F \frac{\partial}{\partial y} \left(\frac{\partial \psi}{\partial y} \right)^2 = 0, \quad (23)$$

$$\frac{\partial^4 \psi}{\partial y^4} - (H^2 + \Omega^2)\frac{\partial^2 \psi}{\partial y^2} + \beta m^2 \frac{\partial \varphi}{\partial y} - C_F \frac{\partial}{\partial y} \left(\frac{\partial \psi}{\partial y} \right)^2 = 0, \quad (24)$$

where the boundary conditions in terms of ψ, the stream function are:

$$\begin{cases} \frac{\partial^2 \psi}{\partial y^2} = 0, \quad \psi = 0, \quad \frac{\partial \theta}{\partial y} = 0 \quad \text{at } y = 0; \\ \frac{\partial \psi}{\partial y} = 0, \quad \psi = F, \quad \theta = 0 \quad \text{at } y = h. \end{cases} \quad (25)$$

Where the wave travelling along the conduit with a height h. Here, additional stream function and boundary conditions are introduced in order to solve the differential equation of order four. The non-dimensional form of the flow rate is defined as $F = Q_0 e^{-At}$, while A and Q_0 are constants. The sign depends upon the constant Q_0. If $Q_0 < 0$, then $F < 0$; similarly $F > 0$ if $Q_0 > 0$. If the flow rate is positive, then it represents the flow is in the direction of peristaltic pumping, however, the direction is opposite, if the flow rate is negative i.e., also known as reverse pumping. It is one of the experimental investigations of Kikuchi [18], that the blood flow rate decreases exponentially with the time rate. Further, it is suggested that the changes in the flow rate are independent of structural details of micro-channel.

4. Solution methodology

In order to get the solution of the higher-order differential equations (22)–(24) first of all these equations are perturbed by using perturbation parameter C_F as it is very small and expressed as:

$$\begin{cases} \psi = \psi_0 + C_F\psi_1 + O(C_F)^2, \\ p = p_0 + C_Fp_1 + O(C_F)^2, \\ \theta = \theta_0 + C_F\theta_1 + O(C_F)^2. \end{cases} \tag{26}$$

4.1. Zeroth order equations

$$\frac{\partial^4\psi_0}{\partial y^4} - (H^2 + \Omega^2)\frac{\partial^2\psi_0}{\partial y^2} + \beta m^2\frac{\partial\varphi}{\partial y} = 0, \tag{27}$$

$$\frac{\partial p_0}{\partial x} = \frac{\partial^3\psi_0}{\partial y^3} - (H^2 + \Omega^2)\frac{\partial\psi_0}{\partial y} + \beta m^2\varphi = 0, \tag{28}$$

$$\frac{\partial p_0}{\partial y} = 0, \tag{29}$$

$$\frac{\partial^2\theta_0}{\partial y^2} + \gamma + Br\left(\frac{\partial^2\psi_0}{\partial y^2}\right)^2 + (H^2 + \Omega^2)Br\left(\frac{\partial\psi_0}{\partial y}\right)^2 = 0, \tag{30}$$

$$\begin{cases} \dfrac{\partial^2\psi_0}{\partial y^2} = 0, \quad \psi_0 = 0, \quad \dfrac{\partial\theta_0}{\partial y} = 0 \quad \text{at } y = 0; \\ \dfrac{\partial\psi_0}{\partial y} = 0, \quad \psi_0 = F, \quad \theta_0 = 0 \quad\quad \text{at } y = h. \end{cases} \tag{31}$$

4.2. First order equations

$$\frac{\partial^4\psi_1}{\partial y^4} - (H^2 + \Omega^2)\frac{\partial^2\psi_1}{\partial y^2} - \frac{\partial}{\partial y}\left(\frac{\partial\psi_0}{\partial y}\right)^2 = 0, \tag{32}$$

$$\frac{\partial p_1}{\partial x} = \frac{\partial^3\psi_1}{\partial y^3} - (H^2 + \Omega^2)\frac{\partial\psi_1}{\partial y} - \left(\frac{\partial\psi_0}{\partial y}\right)^2 = 0, \tag{33}$$

$$\frac{\partial p_1}{\partial y} = 0, \tag{34}$$

$$\frac{\partial^2\theta_1}{\partial y^2} + 2Br\left(\frac{\partial^2\psi_0}{\partial y^2}\right)^2\left(\frac{\partial^2\psi_1}{\partial y^2}\right)^2 + 2(H^2 + \Omega^2)Br\left(\frac{\partial\psi_1}{\partial y}\right)\left(\frac{\partial\psi_0}{\partial y}\right) + Br\left(\frac{\partial\psi_0}{\partial y}\right)^3 = 0, \tag{35}$$

$$\begin{cases} \dfrac{\partial^2\psi_1}{\partial y^2} = 0, \quad \psi_1 = 0, \quad \dfrac{\partial\theta_1}{\partial y} = 0 \quad \text{at } y = 0; \\ \dfrac{\partial\psi_1}{\partial y} = 0, \quad \psi_1 = 0, \quad \theta_1 = 0 \quad\quad \text{at } y = h. \end{cases} \tag{36}$$

Further, the set of differential equations are solved numerically employing Runge–Kutta fourth order method and the iterative procedure of the method is expressed as follows.

Here, Eqs. (27), (30), (32) and (35) behave in the sense of ordinary differential equation with given boundary conditions and the transformation into the set of first order differential equations with initial conditions are as follows.

Let,

$$\psi_0 = y_1, \quad \psi_0' = y_2, \quad \psi_0'' = y_3, \quad \psi_0''' = y_4, \quad \theta_0 = y_5, \quad \theta_0' = y_6.$$

Hence,

$$\psi_0^{iv} = (H^2 + \Omega^2)y_3 - \beta m^2\varphi',$$
$$\theta_0'' = -\gamma - Br\,(y_3)^2 - (H^2 + \Omega^2)Br\,(y_2)^2.$$

Also,

$$\psi_1 = y_7, \quad \psi_1' = y_8, \quad \psi_1'' = y_9, \quad \psi_1''' = y_{10}, \quad \theta_1 = y_{11}, \quad \theta_1' = y_{12}.$$

Therefore,

$$\psi_1^{iv} = (H^2 + \Omega^2)y_9 + 2y_2y_3,$$
$$\theta_1'' = -2Br\,(y_3)^2\,(y_9)^2 - 2(H^2 + \Omega^2)Br\,(y_8)\,(y_2) - Br\,(y_2)^3.$$

And the initial conditions are:

$$\begin{cases} y_3(0) = 0, & y_1(0) = 0, & y_6(0) = 0, & y_9(0) = 0, & y_7(0) = 0, & y_{12}(0) = 0, \\ y_2(0) = s_1, & y_4(0) = s_2, & y_5(0) = s_3, & y_8(0) = s_4, & y_7(0) = s_5, & y_{11}(0) = s_6. \end{cases}$$

However, the assumed initial conditions are obtained using shooting technique and the results are verified till we get a desired accuracy of 10^{-6}.

4.3. Analysis of entropy generation

The intensity of irreversibility that takes place in any thermal procedure is observed by Entropy production. The mathematical expression for the rate of local entropy production is:

$$S_G = \frac{k}{T_w^2}\left[\left(\frac{\partial T}{\partial x}\right)^2 + \left(\frac{\partial T}{\partial y}\right)^2\right] + \frac{1}{T_w}\varphi + \frac{\sigma E_0^2}{T_w} + \frac{\sigma B_0^2}{T_w}\left[u^2 + v^2\right] + \frac{\mu}{k^* T_w}\left[u^2 + v^2\right] +$$
$$\frac{\rho C_{k^*}}{\sqrt{k^*}T_w}\left[\left(u^2 + v^2\right)\sqrt{u^2 + v^2}\right]. \quad (37)$$

The above expression exhibits the dimensional form of entropy production due to thermal irreversibility, irreversibility due to various factors like friction, joule dissipation and porous matrix. The characteristic entropy production is defined as:

$$S_{CG} = \frac{k\left(\frac{qd_h}{k}\right)^2}{T_w^2 d_h^2}. \quad (38)$$

The non-dimensional form of entropy production can be obtained by utilizing Eqs. (37) and (38), and can be stated as:

$$Ns = \frac{S_G}{S_{CG}} = \frac{T_w^2 d_h^2}{k\left(\frac{qd_h}{k}\right)^2}S_G, \quad (39)$$

$$Ns = \left(\frac{\partial\theta}{\partial y}\right)^2 + \frac{1}{\eta}\left[Br\left(\frac{\partial u}{\partial y}\right)^2 + \gamma + \left(H_m^2 + \Omega^2\right)Bru^2 + c_F Bru^3\right]. \quad (40)$$

Total entropy generation in terms of stream function is expressed as:

$$Ns = \left(\frac{\partial\theta}{\partial y}\right)^2 + \frac{1}{\eta}\left[Br\left(\frac{\partial^2\psi}{\partial y^2}\right)^2 + \gamma + \left(H_m^2 + \Omega^2\right)Br\left(\frac{\partial\psi}{\partial y}\right)^2 + c_F Br\left(\frac{\partial\psi}{\partial y}\right)^3\right], \quad (41)$$

where variable η is described as $\eta = [qd_h/kT_W]$. The first term in Eq. (41) denoted as: $N_{tt} = (\partial\theta/\partial y)^2$.

The above expression depicts the production of entropy due to the heat transfer within the conduit. The irreversibility system is dominant over the entropy production number. Bejan number (is defined as the ratio of N_{tt} (thermal irreversibility) to the Ns (total entropy generation)) is used to comprehend the entropy production mechanisms. The Bejan number Be is of the form:

$$Be = \frac{N_{tt}}{Ns} = \left[\frac{\left(\frac{\partial\theta}{\partial y}\right)^2}{\left(\frac{\partial\theta}{\partial y}\right)^2 + \frac{1}{\eta}\left[Br\left(\frac{\partial u}{\partial y}\right)^2 + \gamma + \left(H_m^2 + \Omega^2\right)Bru^2 + c_F Bru^3\right]}\right].$$

The range of the Bejan number is 0 to 1. It is clear that, $Be = 0$ corresponds to the entropy production due to the impacts of several parameters those characterize the entropy. $Be = 0.5$ represents the thermal irreversibility and the irreversibility due to fluid friction, electric field, magnetic field and porous matrix are similar. Thermal irreversibility is dominant when $Be = 1$.

In the present investigation, all these equations are modeled with the consideration of dissipative heat energy. However, in the absence of viscous dissipation, study regarding the contribution of viscous irreversibility in the entropy generation is not considered. Secondly, for $Br = 0$, Bejan number is identically one.

5. Results and discussion

Darcy Forchheimer model for the flow characteristics of peristaltic pumping within a conduit, a channel conveying the biofluid flow, induced by electroosmosis through a non-Darcy porous medium has been considered. In addition to that, magnetic fields, as well as, electric field are applied along the normal and channel direction of the fluid flow, respectively. The required force for electro kinetic flow is produced due to the electric field exerted along the direction of the conduit. The novelty of the present analysis is due to the solution of highly nonlinear coupled transformed governing equations. First, a perturbation technique is used since the equation (24) is of fourth order and due to unavailability of sufficient initial conditions along with equation (23). As a criterion, C_F is introduced as perturbation parameter where $C_F \ll 1$. Henceforth, these equations are reduced to its lower order and still it is a hard task to solve these set of equations analytically, therefore, numerical techniques such as the fourth order Runge–Kutta method in association with shooting technique is employed. Moreover, in the case of peristaltic pumping, the intensity of the irreversibility that takes place in the thermal procedure, the study of entropy generation is also vital. The behavior of the characterizing physical parameter for the pumping with constant pressure gradient on the flow phenomena along with temperature profiles, pressure gradient, entropy and the Bejan number is presented via graphs. In several cases the flow pattern is compared with established results.

5.1. Velocity profiles

The comparison as well as the behavior of several parameters such as Hartmann number, Darcy number and the Forchheimer number is displayed in Fig. 2. Withdrawing the appearance of magnetic field i.e. the absence of Hartmann number, and the Darcy number from the equation (24), the present result validates with the work of Kikuchi [18]. Moreover, the variations of these parameters on the profiles are exhibited. It is a clear indication that, due to the resistance of magnetic field and porosity, the axial velocity decreases in the central region. The fact is, the interaction of the magnetic field in the transverse direction of the axial velocity produces Lorentz force that resists the fluid motion. Further, it is seen that, near the walls of the conduit the effect is reversed. An interesting point to note that the profiles behave with opposite characters from the point of inflection. The behavior of Forchheimer number on the axial velocity is also presented in Fig. 2. However, insignificant enhancement is marked with the increasing Forchheimer number on the velocity profiles. The more hindrance to the flow is marked due to the both Darcy and Forchheimer number. Since, permeability of the porous medium is inversely proportional to both the Darcy and Forchheimer number, higher of these values produces lesser permeability.
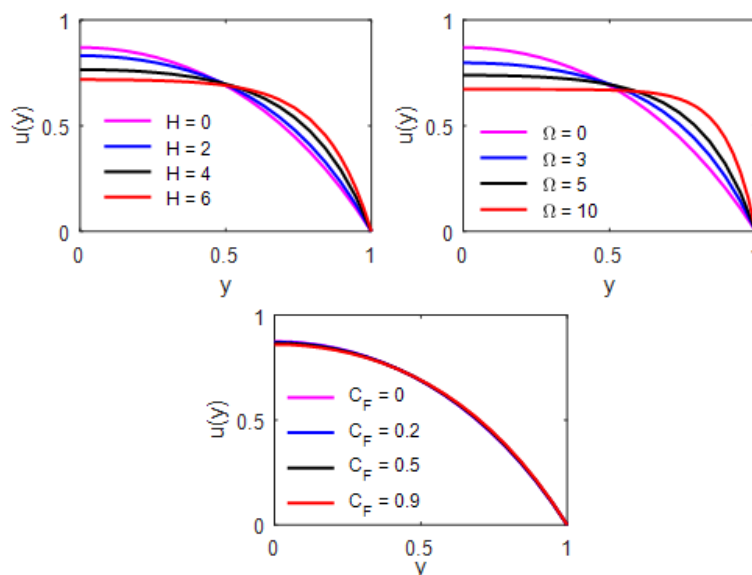

FIG. 2. Velocity profiles for various parameters

5.2. Pumping characteristics

Figure 3 illustrates the characteristic of various physical parameters, such as, Hartmann number, Darcy number, electroosmotic parameter and the Forchheimer number on the peristaltic pumping in the form of pressure gradient. The perception of mechanical pumping is characterized by the peristaltic transport phenomena. From the interaction

of Hartmann numbers it is noteworthy that the magnitude of the pressure gradient increases with increase in Hartmann number. As the conduit is wider than the amount of hike in pressure gradient is less. Therefore, maximum pressure is required for the flow of similar volume of fluid through the channel. Higher Hartmann number produces a stronger Lorentz force and for which more pressure is required to resist the applied force. Moreover, the similar profile is observed due to the enhancement in the values of Darcy number. As similar to the Magnetic field, porosity also a resistive force which enhances the magnitude of pressure gradient. In particular absence of Darcy number, the profile coincides with the earlier established results of Kikuchi [18]. The influence of electroosmosis parameters on the pressure gradient is displayed in Fig. 3. It is defined as the ratio of channel width with the Debye length. However, for lower Debye length values, the pressure gradient with the thickness of the channel decreases. Again the Forchheimer number also affects the pumping characteristics as well which is exhibited in Fig. 3. Both the Darcy and Forchheimer numbers are inversely proportional to each other, described earlier; the symmetrical behavior of the pressure gradient is marked about the middle layer of the channel. Retardation in the profiles is marked throughout the entire domain of the conduit.
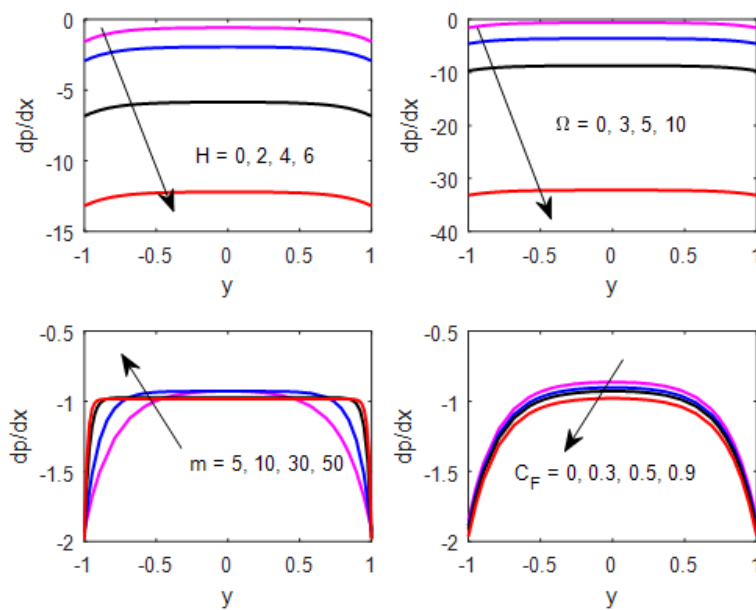

FIG. 3. Peristaltic pumping pressure gradient profile for several parameters

5.3. Temperature profile

In the case of electroosmotic flow, the generation of Joule effect is a built-in characteristic. This is because of the electrolyte. Fig. 4 presents the behavior of the Hartmann number, Joule parameter, Darcy number and the electroosmotic parameter for the fixed values of the other characterizing parameters. It is clear to see that, in the central region of the channel, the temperature of the peristaltic fluid increases due to an increase in Hartmann number. The reason is that, the effect of Lorentz force is stronger in the central region and further the falls in the profile is marked towards the channel walls. This fall in the kinetic energy is accompanied by the enhancement in the thermal energy. Because of brevity, the behavior of the profile is not discussed for entire the region since these are symmetric in nature. Joule heating effect is observed due to the interference of the electric field. It is proportional to the square of the electric field. Therefore, growth in the fluid temperature occurred due to the increase in electric field and is reflected in the central area of the temperature profiles. Moreover, the behavior is insignificant near the walls of the conduit. The impact of the Darcy number is obtained and presented in Fig. 4. It is noteworthy that the profile increases with a higher Darcy number. The boost in the profile is because of the higher Darcy number and the permeability decreases. The behavior of the temperature profile is insignificant for the variation of electroosmotic parameters. Fig. 5 portrays the influence of Brinkmann number and the Forchheimer number on the temperature profiles for the fixed values of other characterizing parameters. Near the center of the conduit, the fluid temperature enhances due to the increase in Brinkmann number. From the definition of Brinkmann number, it is seen that, Boost in the dissipative energy offers higher Brinkmann number and at the same time the molecular conductivity decreases. Because of the same reason, the temperature profile is enhanced. Therefore, it is concluded that, higher Brinkmann number is favorable for enhanced

heat transfer rates.The behavior of Forchheimer parameter on the temperature profile is exhibited in Fig. 5. In the absence of a porous medium, minimum temperature is exhibited within the channel, whereas, higher Forchheimer number is responsible for the lesser permeability of the medium for which the thermal transport enhances.
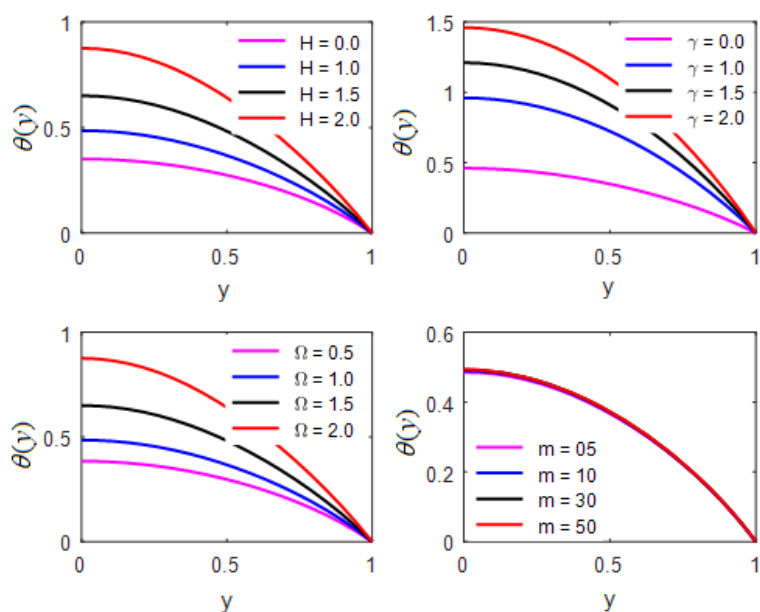

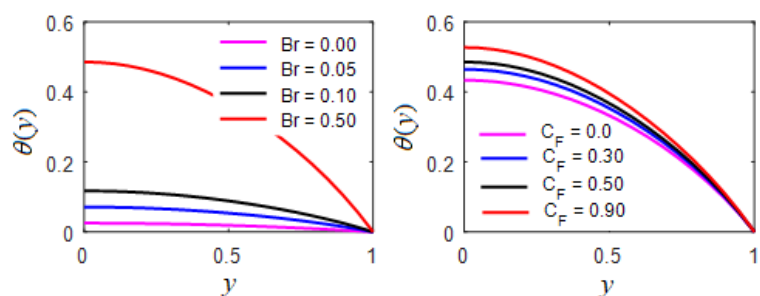FIG. 4. Fluid temperature for contributing parameters

FIG. 5. Fluid temperature for contributing parameters

5.4. Entropy analysis

The thermal energy per unit time is measured by the entropy that is unavailable for doing some useful work due to ordered molecular motion. Its amount also measures the molecular randomness of the system. Fig. 6 elaborates the effects of Joule heating parameter, Hartmann number, Brinkmann number and the Darcy number on the analysis of entropy profiles. It is noted that an increasing Joule heating parameter enhances the value of the entropy near the conduit wall, whereas, at the central region, it becomes linear. Electric field strength helps to enhance the total entropy production. The effect of Hartmann number on the entropy profiles is exhibited in Fig. 6. It is noteworthy that entropy accelerates within the conduit with increasing Hartmann number. In the central area of the channel, due to lesser viscosity the impact is not strong to develop the flow. In the absence of Brinkmann number, i.e., in the case of low viscosity, the amount of entropy is low; as a result, the profile is linear. However, higher Brinkmann numbers produce maximum entropy near the channel wall and in the middle layer it becomes linear. The impact of Darcy number is also similar to that of the behavior of the Hartmann number, as described earlier.
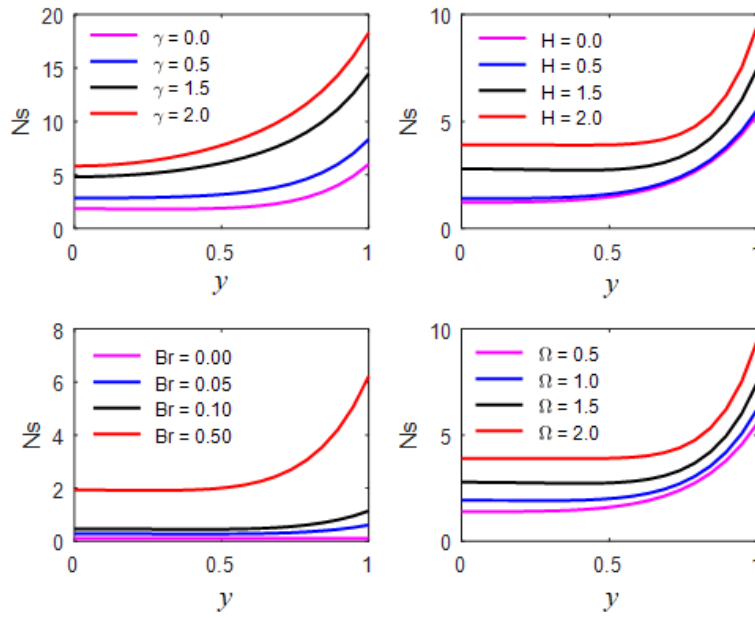
FIG. 6. Entropy production amount for contributing parameters

5.5. Bejan number

Figure 7 portrays the influences of Joule heating parameter, Hartmann number, Brinkmann number and the Darcy number on the Bejan number. It is seen that, for higher values of all these parameters, the growth of the profile is rapid towards the wall of the conduit as the channel width increases. It is obtained by the ratio of heat transfer irreversibility to the total irreversibility due to heat transfer and fluid friction. From the computation, it is clear that the irreversibility of the heat transfer dominates over the total irreversibility for which Bejan number increases. More suitably, Hartmann number and Darcy number favors to enhance the irreversibility processes of the heat transfer.
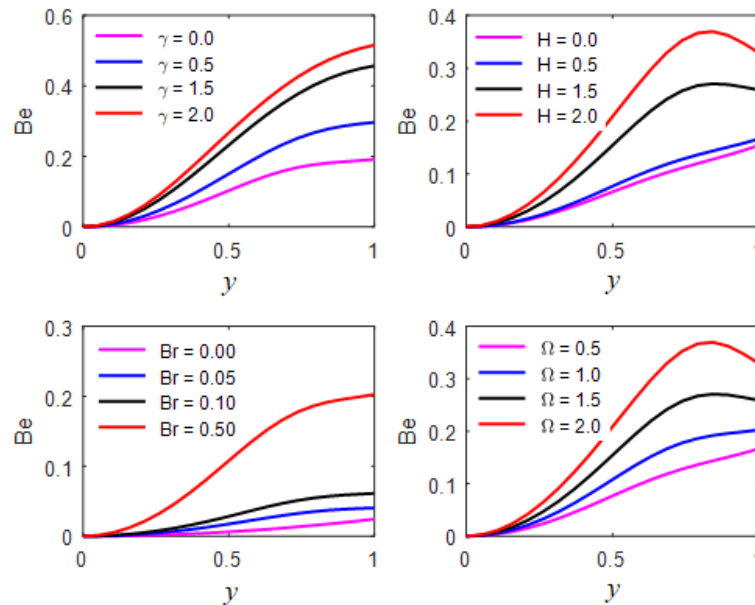

FIG. 7. Bejan number computation for several parameters

6. Conclusion

The current investigation renders in the direction of the electroosmotic flow due to the peristaltic pumping through a non-Darcy conduit in the presence of magnetic field, electric field, Joule heating. The analysis of entropy is also carried out because of the interference of Joule heating. The crux of the present investigation is the solution of a complex partial differential equation in composition with pressure gradient is obtained by both analytically and numerically. A perturbation technique is employed to reduce the PDEs to ODEs and then Runge–Kutta fourth order technique is used to solve the set of transformed ODEs.However, the computation for several contributing parameters are presented via graphs and discussed. The followings are the few concluding remarks from the aforesaid discussions.

- The non-Darcy porous medium and the Hartmann number reduce the axial velocity in the central region of the conduit.
- Electroosmotic parameter boosts the pressure gradient near the channel walls, whereas, in the middle layer, it seems to be steady.
- Interference of Hartmann and Darcy number enhance the fluid temperature.
- Huge amount of Entropy is produced due to the increase of Darcy number and Forchheimer parameter.

7. Nomenclature

ρ_e	density of ionic charge
e	charge of electron
T_{av}	average temperature
δ	wave number
q	heat flux
K_B	Boltzmann constant
Ω^2	Darcy number
H_m	Hartmann number
B_e	Bejan number
Pr	Prandtl number
Br	Brinkman number
C_F	Forchheimer number
γ	joule heating parameter
ν	kinematic viscosity
δ	wave number
Re	Reynolds number
B	mobility of medium
U_{HS}	Helmholtz –Smoluchowski velocity

8. ORCID

Bhimanand Gajbhare https://orcid.org/0000-0002-1911-8602.

References

[1] Bejan A. *Entropy generation minimization*. 2nd ed. Boca Raton: CRC, 1996.

[2] Sciacovelli A., Verda V., Sciubba E. Entropy generation analysis as a design toola review. *Renew Sustain Energy Rev.*, 2015, **43**, P. 1167–1181.

[3] Zhao L., Liu L.H. Entropy generation analysis of electro-osmotic flow in open-end and closed-end micro-channels. *Ain Shams Eng J.*, 2017, **8**, P. 623–632.

[4] Rashidi M.M., Abelman S., Mehr N.F. Entropy generation in steady MHD flow due to a rotating porous disk in a nanofluid. *Int. J. Heat Mass. Transf.*, 2013, **62**, P. 515–625.

[5] Afridi M.I., Qasim M., Khan I., Tlili I. Entropy generation in MHD mixed convection stagnation-point flow in the presence of joule and frictional heating. *Case Stud Therm. Eng.*, 2018, **12**, P. 292–300.

[6] Gul A., Khan I., Makhanov S.S. Entropy generation in a mixed convection Poiseulle flow of molybdenum disulphide Jeffrey nanofluid. *Results Phys.*, 2018, **9**, P. 947–954.

[7] Saqib M., Ali F., et al. Entropy generation in different types of fractionalized nanofluids. *Arab. J. Sci. Eng.*, 2018, **44** (1), P. 1–10.

[8] Adesanya S.O., Falade J.A. Thermodynamics analysis of hydromagnetic third grade fluid flow through a channel filled with porous medium. *Alex Eng. J.*, 2015, **54** (3), P. 615–622.

[9] Afridi M.I., Qasim M., Shafie S., Makinde O.D. Entropy generation analysis of spherical and non-spherical ag-water nanofluids in a porous medium with magnetic and porous dissipation. *J. Nanofluids.*, 2018, **7** (5), P. 951–960.

[10] Abbas M.A., Bai Y., Rashidi M.M., Bhatti M.M. Analysis of entropy generation in the flow of peristaltic nanofluids in channels with compliant walls. *Entropy*, 2016, **18** (3), P. 90.

[11] Rashidi M.M., Bhatti M.M., Abbas M.A., Ali M.E. Entropy generation on MHD blood flow of nanofluid due to peristaltic waves. *Entropy*, 2016, **18** (4), P. 117.

[12] Qasim M., Hayat Khan Z., Khan I., Al-Mdallal Q.M. Analysis of entropy generation in flow of methanol-based nanofluid in a sinusoidal wavy channel. *Entropy*, 2017, **19** (10), P. 490.

[13] Alizadeh R., Karimi N., et al. Mixed convection and thermodynamic irreversibilities in MHD nanofluid stagnation- point flows over a cylinder embedded in porous media. *J. Therm. Anal. Calorim.*, 2018, **135**, P. 489–506.

[14] Shamsabadi H., Rashidi S., Esfahani J.A. Entropy generation analysis for nanofluid flow inside a duct equipped with porous baffles. *J. Therm. Anal. Calorim.*, 2018, **135**, P. 1009–1019.

[15] Cameselle C., Reddy K.R. Development and enhancement of electro-osmotic flow for the removal of contaminants from soils. *Electrochim. Acta*, 2012, **86**, P. 10–22.

[16] Zhou J., Tao Y.L., et al. Electro-osmotic strengthening of silts based on selected electrode materials. *Soils Found.*, 2015, **55** (5), P. 1171–1180.

[17] Tripathi D., Bhushan S., Be'g O.A. Transverse magnetic field driven modification in unsteady peristaltic transport with electrical double layer effects. *Colloids Surf. A*, 2016, **506**, P. 32–39.

[18] Kikuchi Y. Effect of Leukocytes and platelets on blood ow through a parallel array of microchannels: micro-and Macroow relation and rheological measures of leukocytes and platelate acivities. *Microvasc. Res.*, 1995, **50**, P. 288–300.

[19] Tripathi D., Bhushan S., Beg O.A. Transverse magnetic field driven modification in unsteady peristaltic transport with electrical double layer effects. *Colloids Surf. A. Physicochem. Eng. Asp.*, 2016, **506**, P. 32–39.